AN EFFICIENT NUMERICAL SCHEME FOR MODELING TWO-PHASE BUBBLY HOMOGENEOUS AIR-WATER MIXTURES

ARTURO S. LEÓN[1], MOHAMED S. GHIDAOUI[2], ARTHUR R. SCHMIDT[3] and MARCELO H. GARCÍA [4]

[1] Ph.D. Candidate, Dept. of Civil and Envir. Eng., University of Illinois, Urbana, Illinois 61801, USA; Ph: (217)333-6178; Fax: (217)333-0687; Email: asleon@uiuc.edu
[2] Associate Professor, Dept. of Civil Eng., The Hong Kong Univ. of Science and Technology, Hong Kong; Ph: (852)2358-7174; Fax: (852)2358-1534; Email: ghidaoui@ust.hk
[3] Research Assistant Professor, Dept. of Civil and Envir. Eng., University of Illinois, Urbana, IL 61801, USA; Ph: (217)333-4934; Fax: (217)333-0687; Email: aschmidt@uiuc.edu
[4] Chester and Helen Siess Professor and Director of the Ven Te Chow Hydrosystems Lab., Dept. of Civil and Envir. Eng., Univ. of Illinois, Urbana, IL 61801, USA; Ph: (217)244-4484; Fax: (217)333-0687; Email: mhgarcia@uiuc.edu

Abstract

This paper focuses on the formulation and assessment of a second-order accurate Finite Volume (FV) shock-capturing scheme for modeling two-phase water hammer flows using the single-equivalent fluid approximation. The FV formulation of the proposed scheme ensures that mass and momentum are conserved. For achieving a second-order rate of convergence for smooth transients (i.e., flows that do not present discontinuities), a second-order boundary condition is implemented using virtual cells and the theory of Riemann invariants, which is similar to that used for the Method of Characteristics (MOC). Since the two-phase flow governing equations when using the single-equivalent fluid approximation are the same as the one-phase water hammer equations (with exception that the pressure-wave celerity is constant in the latter case), and because analytical solutions are available for the latter case, the numerical efficiency of the proposed model is tested using the one-phase water hammer equations with constant pressure-wave celerity. The validity of the single-equivalent fluid approximation and the proposed scheme herein are verified with laboratory experiments. For one-phase transient flows, numerical tests were performed for smooth and strong transients. For smooth transients, the results show that the efficiency of the proposed scheme is highly superior to the fixed-grid MOC scheme with space-line interpolation and another second-order FV scheme. For one-phase strong transient flows, the results show that the efficiency of the proposed scheme is highly superior to the MOC scheme, and significantly superior to the other FV scheme for coarse grids. For fine grids, the accuracy of the proposed scheme converges to that of the other FV scheme. For two-phase water hammer flows, the results show good agreement between experimental data and the results of numerical simulations.

Introduction

The study of two-phase water hammer flows has great significance in a wide range of industry and municipal applications including power plants, petroleum industries, water distribution systems, sewage pipelines, etc. For modeling these flows, several approaches have been proposed. However, most of these methods are not intrinsically conservative, which means mass and momentum are not conserved. Furthermore, most of these methods are not efficient numerically. The efficiency of the models is a critical factor for Real-Time Control (RTC), since several simulations are required within a control loop in order to optimize the control strategy, and where small simulation time steps are needed to reproduce the rapidly varying hydraulics. RTC is becoming increasingly indispensable for industry and municipal applications in general.

The partial differential equations that describe two-phase flows in closed conduits can be simplified to a great extent when the amount of gas in the conduit is small. In this case, the gas-liquid mixture can be treated as a single-equivalent fluid (e.g., Chaudhry et al. 1990; Martin 1993; Guinot 2001a). The governing equations for the single-equivalent fluid are identical to those for a single-phase flow. Due to this fact, similar techniques to those for a single-phase flow are used to solve simplified models for two-phase flows. However, since shocks may be produced during transient conditions in two-phase flows (i.e., Padmanabhan and Martin 1978), only those methods that can handle shocks without special treatment are suitable for these applications.

In the literature, numerical schemes that have been proposed for modeling one-dimensional two-phase flows using the single-equivalent fluid approximation include MOC schemes, Lax-Wendroff schemes, a plethora of explicit schemes, and implicit methods (e.g., Chaudhry et al. 1990; Martin 1993). Recently, Guinot (2001a, 2001b) has applied Godunov-Type Schemes (GTS) Schemes to two-phase flows with good success. The first-order GTS presented by Guinot (2001a) showed that numerical diffusion leads to a very fast degradation of the quality of the solution after a few oscillation periods. The second-order scheme by Guinot (2001b) is largely superior to his first-order scheme, although an iterative process is required to solve the Riemann problem.

The present paper presents an efficient second-order FV GTS for modeling two-phase water hammer flows. In the proposed scheme, no iteration is required for the solution of the Riemann problem.

Governing equations

The governing equations that describe two-phase flows in closed conduits can be simplified to a great extent when the amount of gas in the conduit is small. In this case, it can be assumed that there is no relative motion or slip between the gas and the liquid and both phases can be treated as a "single-equivalent fluid" with average properties (e.g., Martin 1993). Furthermore, the characteristic time scale of the transients is so small that adsorption/desorption of gas can be considered negligibly small (Zielke et al. 1989). The mass and momentum

conservation equations for the "single-equivalent fluid" assumptions are identical to those for a liquid-phase flow and can be written in their vector conservative form as follows (e.g., Martin 1993):

$$\frac{\partial \mathbf{U}}{\partial t} + \frac{\partial \mathbf{F}}{\partial x} = \mathbf{S} \quad \text{.....(1)}$$

where the vector variable **U**, the flux vector **F** and the source term vector **S** may be written as:

$$\mathbf{U} = \begin{bmatrix} \Omega \\ Q_m \end{bmatrix}, \ \mathbf{F} = \begin{bmatrix} Q_m \\ \frac{Q_m^2}{\Omega} + A_f p \end{bmatrix} \text{ and } \mathbf{S} = \begin{bmatrix} 0 \\ (S_0 - S_f)\rho_f g A_f \end{bmatrix} \quad \text{.....(2)}$$

where ρ_f is the fluid density, A_f is the full cross-sectional area of the conduit, $\Omega = \rho_f A_f$ is the mass of fluid per unit length of conduit, $Q_m = \Omega u$ is the mass discharge, p is the pressure acting on the center of gravity of A_f, g is the gravitational acceleration, S_0 is the slope of the conduit, and S_f is the slope of the energy line. The vector Eq. 1 does not form a closed system in that the flow state is described using three variables: Ω, p and Q_m. However, it is possible to eliminate the pressure variable by introducing the general definition of the celerity of the pressure-wave (a_g), which relates p and Ω:

$$a_g = \left[\frac{d(A_f p)}{d\Omega}\right]^{1/2} \quad \text{.....(3)}$$

The pressure-wave celerity for the gas-liquid mixture (a_m) can be estimated as (Guinot 2001a):

$$a_m = \frac{a}{\sqrt{1 + \psi_{ref}\rho_{f\,ref} a^2 \frac{p_{ref}^{\frac{1}{\beta}}}{p^{\frac{1+\beta}{\beta}}}}} \quad \text{.....(4)}$$

where a is the pressure-wave celerity in presence of liquid only, p_{ref} is a reference pressure for which the density is known ($\rho_{f\,ref}$), β is a coefficient equal to 1 for isothermal processes and 1.4 for adiabatic conditions, and ψ_{ref} is the volume fraction of gas at the reference pressure. The water density measured at a temperature of 4 degrees Celsius under atmospheric pressure conditions is 1000 kg/m^3. Thus, the reference density and pressure when the liquid is water can be taken as 1000 kg/m^3 and 101325 Pa, respectively.

The relationship between the volume fraction of gas ψ and pressure for the "single-equivalent fluid" assumptions can be expressed as (Guinot 2001a):

$$p\psi^{\beta} = p_{ref}\psi_{ref}^{\beta} \quad \text{.....(5)}$$

Substituting Eq. 4 into Eq. 3 and integrating the differentials dΩ and dp (A_f is assumed to be constant) leads to the following equation that relates p and Ω:

$$\Omega = \Omega_{ref} + \frac{A_f}{a^2}\left[p - p_{ref} + (p_{ref}^{\frac{-1}{\beta}} - p^{\frac{-1}{\beta}})\beta\psi_{ref}\rho_{f\,ref}a^2 p_{ref}^{\frac{1}{\beta}}\right] \quad \text{.....(6)}$$

where $\Omega_{ref} = \rho_{f\,ref} A_f$. The pressure p in Eq. 6 is determined by iteration using the Newton Raphson method and typically between three and five iterations are needed to ensure convergence. The flow variables used in this paper are Ω and Q_m. However, the engineering community prefers to use the piezometric head h and flow discharge Q. The latter variables can be determined from Ω and Q_m as follows:

$$Q = \frac{Q_m}{\Omega} A_f \; ; \; h = \frac{p - p_{ref}}{\rho_{f_{ref}} g} + \frac{d}{2} \qquad \text{.....(7)}$$

where h is measured over the conduit bottom. The absolute pressure head (H) in meters of water can be obtained as $H = h + 10.33$.

Formulation of Finite Volume Godunov-type schemes

This method is based on writing the governing equations in integral form over an elementary control volume or cell, hence the general term of Finite Volume (FV) method. The computational grid or cell involves discretization of the spatial domain x into cells of length Δx and the temporal domain t into intervals of duration Δt. The ith cell is centered at node i and extends from $i\text{-}1/2$ to $i+1/2$. The flow variables (Ω and Q_m) are defined at the cell centers i and represent their average value within each cell. Fluxes, on the other hand are evaluated at the interfaces between cells ($i\text{-}1/2$ and $i+1/2$). For the ith cell, the integration of Eq. 1 with respect to x from control surface $i\text{-}1/2$ to control surface $i+1/2$ yields:

$$\mathbf{U}_i^{n+1} = \mathbf{U}_i^n - \frac{\Delta t}{\Delta x_i}(\mathbf{F}_{i+1/2}^n - \mathbf{F}_{i-1/2}^n) + \frac{\Delta t}{\Delta x_i} \int_{i-1/2}^{i+1/2} \mathbf{S} dx \qquad \text{.....(8)}$$

where the superscripts n and $n+1$ reflect the t and $t+\Delta t$ time levels respectively. In Eq. 8, the determination of $\mathbf{U}$ at the new time step $n+1$ requires the computation of the numerical flux ($\mathbf{F}$) at the cell interfaces at the old time n. In the Godunov approach, the flux $\mathbf{F}_{i+1/2}$ is obtained by solving the Riemann problem with constant states $\mathbf{U_i}$ and $\mathbf{U_{i+1}}$. This way of computing the flux leads to a first-order accuracy of the numerical solution. To achieve second-order accuracy in space and time, the Monotone Upstream-centred Scheme for Conservation Laws (MUSCL)-Hancock method is used in this paper. In what follows, an efficient approximate Riemann solver for two phase water hammer flows that does not require iterations is proposed.

Riemann solver for two-phase water hammer flows

In contrast with one-phase water hammer flows, in two-phase flows the pressure-wave celerity may be reduced to very low values, in which case u is not necessarily negligible compared to a_m. However, u is still smaller than a_m and consequently the characteristics travel in opposite directions and the star region ($*$), which is an intermediate region between the left and right states, contains the location of the initial discontinuity. Thus, the flow variables in the star region are used to compute the flux. Simple estimates for (Ω_* and Q_{m*} that do not require iterations can be obtained by solving the Riemann problem for the linearized hyperbolic system $\partial \mathbf{U}/\partial t + \partial \mathbf{F}(\mathbf{U})/\partial x = 0$ that yields:

$$\Omega_\star = \left(\frac{\Omega_L + \Omega_R}{2}\right)\left(1 + \frac{u_L - u_R}{2\bar{a}_m}\right); \quad Qm_\star = Qm_L + (\bar{u} - \bar{a}_m)(\Omega_\star - \Omega_L) \qquad \text{.....(9)}$$

where $\bar{a}_m = (a_{m\,L} + a_{m\,R})/2$ and $\bar{u} = (u_L + u_R)/2$. By using the estimated values of Ω_* and Q_{m*}, the flux is obtained from Eq. 2.

Second-order accurate boundary conditions

For the quality of the numerical solution to be preserved, it is necessary to use the same order of reconstruction in all the cells of the computational domain (e.g., Guinot 2003). The MUSCL-Hancock scheme uses one cell on each side of the cell in which the profile is to be reconstructed. Therefore, one cell is missing when the profile is to be reconstructed within the first and last cells of the computational domain. The missing information at the boundaries is restored by adding one virtual cell at each end of the computational domain. The virtual cell on the left-hand side is numbered *0*, while the cell on the right-hand side of the domain is numbered *Nx+1*. The algorithm consists of the following steps: (1) determination of **U** at the boundaries *1/2* and *Nx+1/2*, and (2) determination of the average flow variables **U** over the virtual cells. The first step used in this paper is the same as in Guinot (2003). The second step is presented next.

Determination of U in the virtual cells

Virtual cells are used only to achieve second-order accuracy in the first and last cells of the computational domain. Therefore, they should advect the same outflowing information as that at the boundaries and they should maintain the conservation property of the shock capturing scheme. The latter means that no unphysical perturbations into the computational domain may be introduced by the virtual cells. These constraints may be satisfied: (1) by assuming that the outflowing wave strengths in the virtual cells are the same as those at the boundaries, and (2) by adjusting the inflowing wave strengths in the virtual cells in such a way that the fluxes in these cells are the same as those at the respective boundaries. For the left hand boundary, a simple formulation that satisfies these two conditions is given by:

$$\Omega_0^{n+1} = \Omega_{1/2}^{n+1/2} = \Omega_b^{n+1/2}$$
$$Q_{m0}^{n+1} = Q_{m1/2}^{n+1/2} = Q_{mb}^{n+1/2} \quad \text{.....(10)}$$

Note that the inflowing and outflowing fluxes in the cell *0* are the same, which means that no perturbations are introduced from the virtual cells into the computational domain when updating the solution. Notice also that with this formulation, the outflowing information advected by the virtual cells is the same as that at the boundaries.

Evaluation of the model

The two-phase flow governing equations when using the single-equivalent fluid approximation are the same as the one-phase water hammer equations (with exception that the pressure-wave celerity is constant in the latter case). Because analytical solutions are available for the latter case, the numerical efficiency of the proposed model is tested using the one-phase water hammer equations with constant pressure-wave celerity. The efficiency of the proposed method for smooth and strong transients is investigated using analytical solutions, the fixed-grid MOC scheme with space-line interpolation, and the second-order scheme of Zhao and Ghidaoui (ZG) [2004]. The validity of the single-equivalent fluid approximation and the proposed scheme herein are verified with laboratory experiments.

In the following sections, the number of grids, grid size and Courant number used in each example are indicated in the relevant figures and thus will not be repeated in the text. The CPU times that are reported in this paper were averaged over three realizations and computed using a HP AMD Athlon (tm) 64 processor 3200 + 997 MHz, 512 MB of Ram notebook.

Test 1: Gradual and partial, and instantaneous downstream valve closure in a frictionless horizontal pipe (one-phase flow)

This test is used to compare the numerical efficiency of the proposed scheme with the second-order scheme of ZG (2004) and the MOC scheme with space-line interpolation for smooth transients (i.e., flows that do not present discontinuities) and strong transients. The test considers one horizontal frictionless pipe connected to an upstream reservoir and a downstream valve. Because of the absence of friction, any dissipation or amplification in the results is solely due to the numerical scheme. The length of the pipe is 10000 *m* and its diameter is 1.0 *m*, the pressure-wave celerity is 1000 *m/s*, the upstream reservoir constant head h_0 is 200 *m*, and the initial steady-state discharge is 2.0 m^3/s. For the case of smooth transients, the flow is obtained after a gradual and partial closure of the downstream valve. For simplicity, this valve is ideally operated in such a way that the flow discharge at the valve is given by the following relationship:

$$Q_b(m^3/s) = \begin{bmatrix} 2*(1-0.3t/20) & \text{for t} < 20 \text{ s} \\ 1.4 & \text{for t} \geq 20 \text{ s} \end{bmatrix}$$

As suggested by Ghidaoui et al. (1998), the energy equation of Karney (1990) can be used to obtain a quantitative measure of numerical dissipation. The energy equation of Karney states that the total energy (sum of internal and kinetic) can only change as work is done on the conduit or as energy is dissipated from it. In this test the friction is set to zero, so the rate of total energy dissipation is zero. At the downstream boundary, fluid is exchanged with the environment across a pressure difference; therefore work is produced at this boundary. At the upstream boundary, the head at the reservoir is the same as the head after the transient flow has reached steady state. Thus, no work is produced at the upstream end of the pipe (see Karney 1990). Because work is produced at the downstream boundary, the total energy (sum of kinetic and internal) is not invariant with time. Rather it changes periodically with time.

Figure 1 shows relative energy traces for the schemes under consideration. The relative energy is expressed as $(E - E_s)/(E_{0p} - E_s)$, where E_{0p} is the total energy after the flow discharge at the valve is constant (e.g., first energy peak in Fig. 1), E_s is the total energy after flow has reached steady state (i.e., by numerical dissipation) and E is the total energy at any time. Figure 1 shows clearly a reduction in the relative energy as the valve is gradually closed until the flow discharge at the valve is constant ($t <= 20$ *s*). For $t > 20$ *s*, the energy plot changes periodically with the same frequency of the water hammer flow. If numerical dissipation would be zero, the energy peaks in Figure 1 must be maintained. Thus, the numerical dissipation (accuracy error) can be obtained as follows:

$$\text{Num. dissipation} = 1 - \frac{E - E_s}{E_{0p} - E_s} = \frac{E_{0p} - E}{E_{0p} - E_s}$$

In this way, if $E = E_{0p}$ there is no numerical dissipation. Likewise, if $E = E_s$ (steady state), the numerical dissipation is 100 %. The evaluation of E is made at the ninth energy peak in Fig. 1 (t ≈370 s).

An objective comparison of efficiency requires measuring the CPU time needed by each of the schemes to achieve the same level of accuracy (i.e., ZG 2004, León et al. 2005). To compare the efficiency of the schemes, the numerical dissipation is plotted against the number of grids on log-log scale and shown in Fig. 2. In this figure, the reduction in numerical dissipation when the number of grids is increased can be approximated as piecewise linear (on log-log scale). Therefore, for a range of *Nx*, the relationship between numerical dissipation and *Nx* can be fitted to power functions of the form $(E_{0p} - E)/ (E_{0p} - E_s) = c_1 Nx^{c2}$. In this power function form, *c2* represents the rate of convergence of the scheme. The power functions presented in Fig. 2 show that the rate of convergence of the proposed scheme is second-order, however the order of convergence of the MOC scheme and the second-order scheme of ZG (2004) are at most only first-order.

For comparison of CPU times, five levels of accuracy error were selected (0.5% - 10%). The number of grids needed by each of the schemes to achieve the five levels of accuracy error were obtained from Fig. 2, and when necessary using the power functions shown in this figure. These number of grids in turn were used to compute the CPU times. The accuracy error against the CPU time is plotted and shown in Fig. 3. For the conditions presented in Fig. 3, it is found that the proposed scheme is about 9 to 2100 times faster to execute than the MOC scheme, and 10 to 15200 times faster than the scheme of ZG. The difference in efficiency of the proposed scheme with respect to the other two schemes becomes much more important when convergence is close to being achieved. The proposed scheme is less dissipative (more accurate) than that of ZG because a second-order boundary condition is used in the proposed approach and only a first-order boundary condition in the second-order scheme of ZG.

Due to space limitations, the results for strong transient flows that were obtained after an instantaneous closure of the downstream valve, the results are not presented, however the main findings are summarized below:

The rate of convergence of the MOC scheme is smaller than that of ZG and the proposed scheme. Among the last two approaches, for relatively coarse grids, the rate of convergence of the scheme of ZG is greater than that of the proposed scheme, however the accuracy of the proposed scheme is superior to that of ZG. For relatively fine grids, the rate of convergence of the scheme of ZG converges to that of the proposed scheme, and the accuracy of the proposed scheme converges to that of ZG. Overall, for levels of accuracy between 1% - 15%, it is found that the proposed scheme is about 30 to 1600 times faster to execute than the MOC scheme, and 5% to 17% faster than the scheme of ZG.

Test 2: Comparison with two-phase flow experiments of Chaudhry et al. (1990)

To verify the validity of the two-phase flow model and the proposed scheme presented herein, one of the sets of experiments conducted at the hydraulics laboratory of the Georgia Institute of Technology in 1990 was considered as the test case. The schematic of the test facility is shown in Fig. 4. Two sets of these experiments were reported in Chaudhry et al. (1990). The second set of experiments is used in this paper.

The test procedure was as follows: A steady state flow of an air-water mixture was established in the test pipe by controlling the exit valves and the pressure of the injected air at the inlet. The air-water mixture flow velocity was maintained at a high enough rate so that slug flow could be avoided by limiting the rate of air injection. Transient flow was created by a rapid valve closure at the downstream end of the pipe. Transient-state pressures were monitored by high-frequency-response pressure transducers at three locations (1, 2 and 3), as shown in Fig. 4. The three stations were located at x = 8 m, 21.1 m and 30.6 m, respectively, from the upstream end.

The upstream boundary was a constant-level reservoir while the downstream boundary was the recorded pressure history at station 3 (x = 30.6 m). A flow discharge boundary condition was not used at the downstream end because the rate of closure of the exit valve was not reported in Chaudhry et al. (1990). They suggested instead to use the recorded pressure history at station 3 as downstream boundary condition because the measurement of the rate of closure of a valve and, consequently the measurement of velocity or discharge is very difficult. The simulated pressures traces at stations 1 and 2 assuming isothermal conditions (β = 1) are contrasted with the corresponding experimental observations in Figures 5(a) and 5(b). As shown in these figures, the experimental pressure traces are satisfactorily reproduced. Chaudhry et al. (1990) and Hadj-Taïeb and Lili (2000) presented graphical comparisons of their numerical results with experimental data of Chaudhry et al. (1990). Qualitatively, the agreement between experimental data and numerical results presented herein is better than that reported in Chaudhry et al. (1990) and Hadj-Taïeb and Lili (2000). The small discrepancies between simulated and observed values may be attributed to experimental uncertainty, unsteady friction, and due to the fact that the process is not necessarily isothermal as was considered in the simulations. Furthermore, gas release and solution processes may not be negligible for damping estimation (Cannizzaro and Pezzinga 2005).

Conclusions

This paper focuses on the formulation and assessment of a FV second-order accurate shock-capturing scheme for modeling two-phase water hammer flows using the single-equivalent fluid approximation. The key results are as follows:

1. FV formulation ensures that the proposed scheme herein conserves mass and momentum.
2. Numerical tests for one-phase (constant pressure-wave celeriy) flow were performed for smooth and strong transients. For smooth transients (i.e., flows that do not present

discontinuities) the results show that the rate of convergence of the proposed scheme is second-order, and at most only first-order for the second-order GTS scheme of ZG (2004) and the MOC scheme. The results also show that to achieve a given level of accuracy, the efficiency of the proposed scheme is highly superior to both, the MOC scheme and the scheme of ZG. For one-phase strong transient flows, the results show that the efficiency of the proposed scheme is highly superior to the MOC scheme, and significantly superior to the other FV scheme for coarse grids. For fine grids, the accuracy of the proposed scheme converges to that of the other FV scheme. For two-phase flows, good agreement between experimental data and the results of numerical simulations is obtained.

Acknowledgments

The authors gratefully acknowledge Dr. C. Samuel Martin for providing us his two-phase flow experimental data and Dr. Ming Zhao for providing us his one-phase water hammer and MOC codes. The financial support of the Metropolitan Water Reclamation District of Greater Chicago (MWRDGC) is also gratefully acknowledged.

References

Cannizzaro, D., and Pezzinga, G. (2005). "Energy dissipation in transient gaseous cavitation." *J. Hydraul. Eng*., 131(8), 724-732.

Chaudhry, M. H., Bhallamudi, S. M., Martin, C. S., and Naghash, M. (1990). "Analysis of transient in bubbly homogeneous, gas-liquid mixtures." *J. Fluids Eng.*, 112, 225-231.

Chaudhry, M. H., and Hussaini, M. Y. (1985). "Second-order accurate explicit finite-difference schemes for water hammer analysis." *J. Fluids Eng.*, 107, 523-529.

Ghidaoui, M. S., Karney, B. W., and McInnis, D. A. (1998). "Energy estimates for discretization errors in water hammer problems." *J. Hydraul. Eng.*, 124(4), 384-393.

Guinot, V. (2001a). "Numerical simulation of two-phase flow in pipes using Godunov method." *Int. J. Numer. Meth. in Eng.*, 50, 1169-1189.

Guinot, V. (2001b). "The discontinuous profile method for simulating two-phase flow in pipes using the single component approximation." *Int. J. Num. Meth. Fluids*, 37, 341-359.

Guinot, V. (2003). *Godunov-type schemes*, Elsevier Science B.V., Amsterdam, The Netherlands.

Hadj-Taïeb E., and Lili, T. (2000). "Validation of hyperbolic model for water hammer in deformable pipes." *J. Fluids Eng.*, 122, 57-64.

Karney, B. W. (1990). "Energy relations in transient closed-conduit flow." *J. Hydraul. Eng.*, 116(10), 1180-1196.

León A. S., Ghidaoui, M. S., Schmidt, A. R., and García M. H. (2005). "Importance of numerical efficiency for real time control of transient gravity flows in sewers." *Proc., XXXI IAHR Congress*, Seoul, Korea.

Martin, C. S. (1993). "Pressure-wave propagation in two-component flow." *Proc., Computer modeling of free-surf. and press. flows*, NATO ASI Series E, Applied Sciences Vol. 274,

Pullman, WA, U.S.A., 519-552.

Padmanabhan, M., and Martin, C. S. (1978). "Shock-wave formation in flowing bubbly mixtures by steepening of compression waves." *Int. J. Multiphase Flow*, 4, 81-88.

Zielke, W., Perko, H. D., and Keller, A. (1989). "Gas release in transients pipe flow." *Proc., 6th Int. Conf. on Pressure Surges*, BHRA, Cambridge, England, Oct. 4-6, 3-13.

Zhao, M., and Ghidaoui M. S. (2004). "Godunov-type solutions for water hammer flows." *J. Hydraul. Eng.*, 130(4), 341-348.

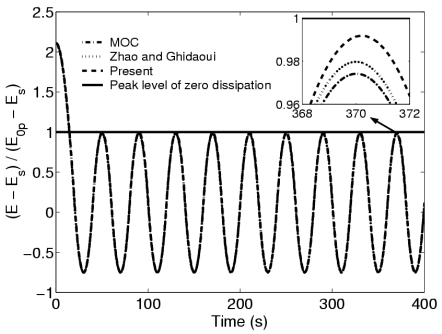

Fig. 1 Energy traces for test No 1 ($Nx = 40$ cells, $\Delta x = 250$ *m*, $Cr = 0.8$)

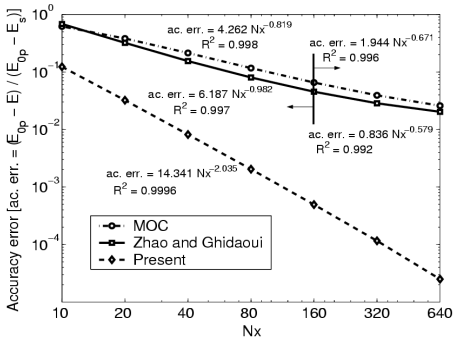

Fig. 2 Accuracy error versus number of grids for test No 1 ($t \approx 370$ s, $Cr = 0.8$)

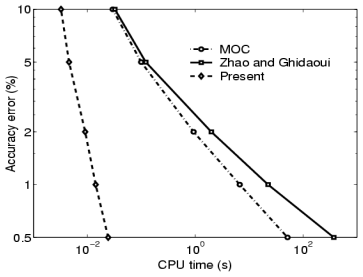

Fig. 3 Relation between level of accuracy and CPU time for test No 1 ($t = 370$ *s*, $Cr = 0.8$)

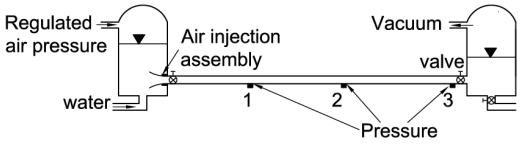

Fig. 4 Schematic of experiment Chaudhry et al. (1990)

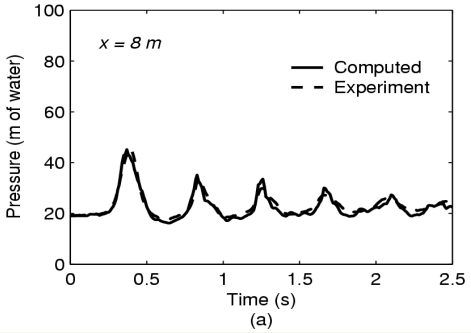

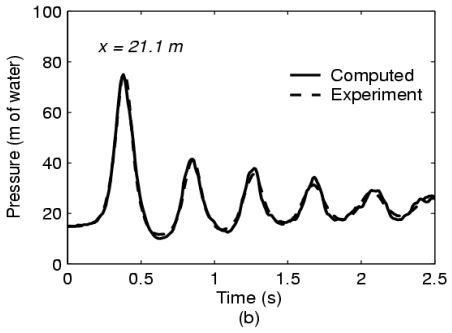

Fig. 5 Computed and experimental absolute pressure traces (a) at $x = 8$ *m* and (b) at $x = 21.1$ *m* ($Nx = 100$ cells, $\Delta x = 0.306$ *m* and $Cr = 0.8$).